The Journal of Applied Sciences Research

Journal homepage: http://www.journals.wsrpublishing.com/index.php/tjasr

Online ISSN: 2383-2215 Print ISSN:2423-4400

Original Article

Predicting the Performance of Artificial Barrier Fracturing with the Aid of Neural Network Modeling

Ahmed A. Elgibaly[1], Mohsen. G. K. El-Nouby[2], Mahmoud A. A. El-Fattah[3]

[1]Faculty of Petroleum and Mining Engineering, Suez University, Egypt
[2] Faculty of Petroleum and Mining Engineering, Future University, Egypt
[3] Qarun Petroleum Company, Egypt

ABSTRACT

Fracture geometry and conductivity are critical parameters for fracture treatment optimization, especially in cases that close to unwanted zones either water-bearing or gas zones. This study investigates the Artificial Neural Network (ANN) model for hydraulic fracturing optimization. The workflow begins with an integrated ANN model, then sets of variable fracture parameters and formation rock properties were utilized for training and testing the ANN based on the most appropriate activation function, the number of hidden layers and the number of neurons. The ANN model considers a 59 real field data of hydraulic fracturing treatments across the western desert of Egypt. The proposed ANN trained based on pressure transient test analysis that was conducted on the real field data. The available data was divided as 70% for training, 15% for validation, and 15% for testing. The optimum number of hidden layers and neurons was achieved after several trials. The proposed ANN model result was promising as compared with the common fracture simulation software FracCade^{TM}. The cross plot of the actual fracture geometry parameters versus the predicted ANN outputs showed a good match with the correlation coefficient (R) for the whole data is 0.93. Then the relative importance of the ANN input parameter on the fracture geometry optimization was employed by the Garson method. The result of this work shows the potential of the approach developed based on the ANN model for predicting the fracture geometry.

Keywords: Artificial Barrier Fracturing, Artificial Neural Network, MATLAB, hydraulic fracture optimization.

ARTICLE INFO

Corresponding Author: Mahmoud A. A. El-Fattah < mahmoud_ali_abd_el_fatah@yahoo.com >

How to Cite this Article: Elgibaly, A.A., El-Nouby, M.G.K., El-Fattah, M.A.A. (2020). Predicting the Performance of Artificial Barrier Fracturing with the Aid of Neural Network Modeling. *The Journal of Applied Sciences Research*, 7(1), 69-86.

Article History: Received: 2020-07-10 Accepted: 2020-08-18

NOMENCLATURE

A/R"G	ABU ROASH G Formation	PBU	Pressure build-Up Test
BHP	Bottom hole pressure, [psi]	P	Internal fracture pressure, [psi]
Cl.G.	Closure gradient, [psi/ft]	Q	Fluid injection rate, [bpm]
E	Young's modulus, [psi]	WOC	Water oil contact
F.G.	Fracture gradient [psi/ft]	WON	West of Nile
Hf	Fracture height, [ft]	W	Fracture width, [in]
ISIP	Instantaneous shut in pressure, [psi]	Xf	Fracturing half-length, [ft]
K	Fracture permeability, [md]	v	Poisson ratio
k	Formation permeability, [md]	σmin	Minimum in-situ stress, [psi]
MAWHP	Max allowable wellhead pressure, [psi]	n′, k′	Power-law fluid coefficients
MD	Measured depth, [ft]	E ′	Plane strain modulus
PNet	Net pressure, [psi]	σ(y)	Horizontal tectonic stress, [psi]

INTRODUCTION

Hydraulic fracturing is usually utilized to create enhanced wellbore connectivity to help tight reservoirs to produce hydrocarbon. Several factors may be considered as risks to the success of fracturing treatment operations. One of the risks arises in pay zone reservoirs that are near to a water-bearing zone. The chance of fracture growth into the water zone limits the stimulation options and decreases the possibilities of using hydraulic fracturing treatment to improve well productivity, thereby limiting the well's future production, decrease recovery factor, and often leading to lost recoverable reserves.

Many of the wells at the western desert of Egypt are shut-in due to poor productivity and often the companies that used artificial lift produce with little recovery. In common terms, these are thought-about to be marginal wells and not worthy for specific attention [1]. In addition to several wells were to be fracture stimulated with a risk of growth through a nearby water zone. The productive pay of tight reservoirs is separated from underlying water zones by a weak or no stress barrier. The distance between the water bearing zone to the pay zone was 20 to 80 ft (Salah *et al.*, 2016).

Controlling the fracture height in such well conditions to stop the fracture growth into the underlying water zone becomes a significant challenge. This may gamble the post-treatment well productivity. Thus it becomes necessary to prevent fracture height propagation from growing into the neighboring water zone, to eliminate the risk of lost well productivity, then reserves.

An Artificial neural network model was developed to predict the fracture geometry as output by using the backpropagation method for different cases in the western desert of Egypt (Mutalova *et al.*, 2019). Based on several input data for interested zone rock properties, overlying and underlying formations, fracture design parameters, and well test data, it can optimize the fracture treatment especially in cases close to water-bearing zones.

The objective of this study was to develop a new model to have the ability to

- Predict and optimize the fracture height to limit the height growth into unwanted zones.
- Predict the effective fracture half-length in tight reservoirs to optimize the fracture treatment
- Calculate dimensionless fracture conductivity (FCD) for fracture treatment to maximize the well productivity.
- Integrating all of the stress profile, fluid, proppant properties, fracture pumping parameters, and the previous well test data to optimize the upcoming fracture treatment.

- Evaluate which parameter has a high effect on fracture geometry based on each input weight.
- Give high accuracy outputs compared to commercial software, therefore eliminate the need for well testing if not available to conduct well testing.

The neural network model has the ability to collect all of the above-desired characteristics because of its ability to handle complex and nonlinear problems (Mutalova *et al.*, 1996). ANN can be trained to know how much the correlative pattern between variables, therefore can be used to predict outputs from new inputs parameter.

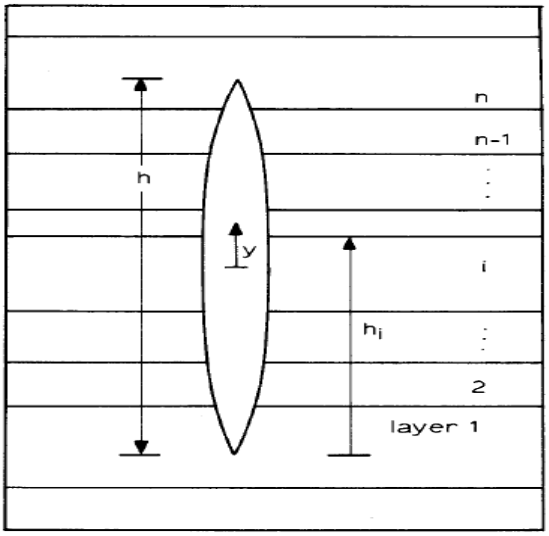

Fig. 1- Definition of variables for fracture containment problem (Fung *et al.*, 1987).

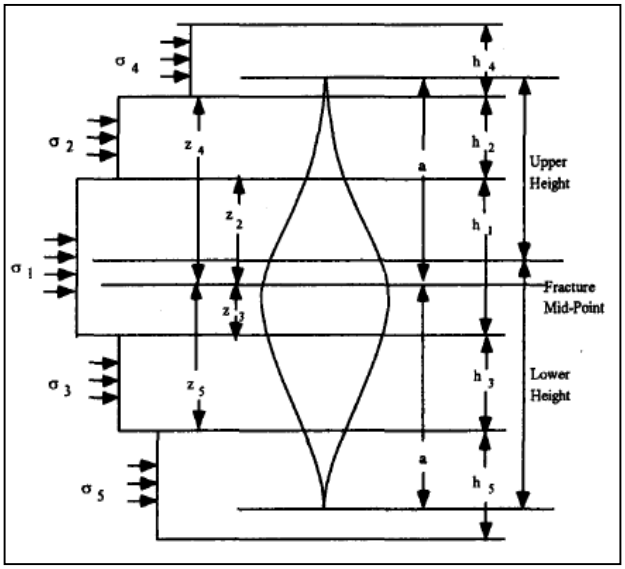

Fig. 2- Hydraulic fracture propagation in multi-stress layers (Rahim and Holditch, 1993).

LITERATURE REVIEW

Over the years, several authors have proposed the optimization of hydraulic fracture treatment by optimizing the fracture geometry and conductivity to maximize well productivity. Usman *et al.*, (Ahmed, 1984) provided a pseudo-3D model through the fracture mechanics equation with the assist of either Geertsma & Deklerk and Perkin & Kern 2D models for accounting fracture geometry. The feature of this model lies in the capability of integrating rock and fluid properties with fracture parameters of symmetry layers above and below the pay zone in the reservoir.

Fung *et al.*, (Fung *et al.*, 1987) state that reservoir properties and tectonic stress are not symmetric and introduce mathematical fracture penetration formula for computing vertical fracture growth in homogeneous reservoirs with horizontal stress distribution as illustrated in Fig. 1. Eq. 1 can be used to solve for the pressure p, which will yield the fracture of height h, once the fracture height that satisfies Eq. 2 is obtained.

$$\mathbf{F_{\sigma m}} = \sqrt{\frac{2}{\pi h}}\left\{(\mathbf{p}-\boldsymbol{\sigma_n})\boldsymbol{\pi} + \sum_{i=1}^{n}(\boldsymbol{\sigma_{i+1}}-\boldsymbol{\sigma_i}) \times \left[\mathbf{2}\sin^{-1}\sqrt{\frac{2h_i}{i}} - (-1)^m\sqrt{1-\left(\frac{2h_i-h}{h}\right)^2}\right]\right\} \quad \text{.....(1)}$$

$$\mathbf{F_\sigma} = \mathbf{F_{\sigma p}} + \mathbf{F_{\sigma\sigma}} \quad \text{.....(2)}$$

where m is 1 or 2 for the lower and upper tips, respectively,

$\mathbf{F_{\sigma p}}$ = internal fracture pressure,

$\mathbf{F_{\sigma\sigma}}$ = Tectonic Loading

Rahim *et al.*, (1993) present a mathematical equation for computing the approximate value of fracture height either up or down growth that can be after that use as an input for the PKN-2D model to evaluate the fracture half-length and dimensionless fracture conductivity. Rahim considers asymmetric layers where the stress difference between upper and lower layers is equal with a given value of net pressure and reasonable values of zones thickness, fracture toughness Fig. 2.

For a given number of layers, the mathematical formula as following:

$$\frac{\sqrt{\pi\alpha}(K_{icn}-K_{icm})}{2}=\sum_{i=1,2}^{m}S_i\sqrt{\alpha^2-Z_i^2}-\sum_{j=3,2}^{n}S_j\sqrt{\alpha^2-Z_j^2} \quad \text{.....(3)}$$

and

$$\frac{\sqrt{\pi\alpha}(K_{icm}-K_{icn})}{2\sqrt{\alpha}}=\sum_{i=1,2}^{m}\sin^{-1}\left(\frac{Z_i}{\alpha}\right)+\sum_{j=3,2}^{n}\sin^{-1}\left(\frac{Z_j}{\alpha}\right)+\frac{S_o\,\pi}{2} \quad \text{.....(4)}$$

$$h_u = \alpha - Z_2 + \frac{h_1}{2} \quad \text{.....(5)}$$

$$h_d = 2\alpha - h_u \quad \text{.....(6)}$$

where

h_u = Upper fracture height,

h_d = Down fracture height,

m = Number of upper layers in which fracture will propagate,

n = Number of lower layers in which fracture will propagate.

Yang *et al.*, (2011) introduce an alternative technique to calculate fracture geometry by using the concept of Unified fracture Design (Economides *et al.*, 2002) proppant number with the Pseudo-3D model. Yang started his approach by assuming net pressure value, then the fracture height was calculated by the equilibrium height calculation. The fracture height with proppant mass and permeabilities of reservoirs result in getting the value of proppant number which in turn evaluates the value of fracture half-length and width. The 2D fracture propagation model can be used to calculate the value of net pressure which was compared with the assumed value.

Garavand *et al.*, (2018) suggest a combination of a unified fracture design concept, a 2D model and a linear elastic fracture mechanic (LEFM) to calculate the fracture geometry. This combination called Modified Pseudo-3D Model.

First, the linear elastic fracture mechanic used to estimate equilibrium fracture height related to pressure, in-situ stress, and fracture toughness distribution. Therefore, UFD with the 2D model was used to calculated fracture half-length and Pnet. This approach covers more variety of multi-layered reservoirs with real in-situ stress distribution than the Yang approach. Both approaches were programmed through MATLAB™ Software.

Table 1 presents the different approaches of the previous authors to optimize the fracture geometry and control fracture height from propagation into unwanted zones. There were several approaches such as Mendelsohn *et al.*, (1984), Palmer and Luiskutty (1986), and Ahn *et al.*, (2017) that present various models for hydraulic fracture propagation. All of these authors did not consider the artificial barrier mass proppant, proppant pack permeability, and proppant type effects in their approaches.

Artificial Neural Network (ANN) model was developed to predict hydraulic fracture height, fracture half-length, and dimensionless fracture conductivity as outputs by using backpropagation for different cases in the western desert of Egypt and west of Nile fields.

DATA USED

The real data used in this study were collected from different fields in the western desert of Egypt and the west of Nile. The data were divided into three categories: formation rock properties, fracture treatment pumping parameters, and pressure transient analysis data Table 2. The real pressure data were measured from downhole memory gauges. Table 3 presents the data range for 59 hydraulic fracturing treatments.

ANN MODEL DEVELOPMENT

In order to build the ANN model for prediction fracture height, half-length, and dimensionless fracture conductivity, the model was passed through 4 stages as following (Elkatatny, 2018):

- Data Preprocessing,
- Normalizing data set,
- Model learning,
- Model evaluation.

Data Preprocessing

Table 2 illustrate the input data for ANN. Among 49 data sets as input parameter across 59 well were including formation rock properties for an interested zone like in-situ stress, young's modulus and fracture toughness, formation data like permeability, porosity and reservoir pressure, mini frac analysis data like net pressure, ISIP, closure gradient and hydraulic fracturing parameters like pumping rate, gel load, proppant mass volume.

Table 1: Different approaches for hydraulic fracture optimization

No.	Authors	Model Type	Objective Function	Ignored parameters
1	Usman et al., (1984)	3D and 2D Model	• Vertical fracture height • Fracture half-length • Fracture width	• Artificial Barrier mass proppant • Artificial Barrier Proppant Pack permeability • Proppant type
2	Fung et al., (1987)	Mathematical Model	• Vertical fracture height	• Artificial Barrier mass proppant • Artificial Barrier Proppant Pack permeability • Proppant type
3	Rahim et al., (1993)	Mathematical Model	• Vertical fracture height • Fracture half-length • Fracture width • Dimensionless fracture conductivity	• Artificial Barrier mass proppant • Artificial Barrier Proppant Pack permeability • Proppant type
4	Yang et al., (2011)	Pseudo-3D Model	• Vertical fracture height • Fracture half-length • Fracture width	• Artificial Barrier mass proppant • Artificial Barrier Proppant Pack permeability • Proppant type
5	Garavand et al., (2018)	Modified Pseudo-3D (LEFM and 2D-UFD) Model	• Vertical fracture height • Fracture half-length • Fracture width	• Artificial Barrier mass proppant • Artificial Barrier Proppant Pack permeability • Proppant type
6	Present work	ANN	• Vertical fracture height • Fracture half-length • Dimensionless fracture conductivity	

Normalizing data set

A spatial database was built consisting of 59 real field data covering almost the western desert of Egypt and west of Nile fields. All explanatory factors for rock and fracture treatment properties were added into the database. Normalization indicates that all the connection weights and the neuron activation thresholds are initialized with small random values, to achieve consistent results through learning. This was performed by the following scaling rule (The Egyptian General Petroleum Corporation, 1992):

$$\mathbf{T_{new}} = \frac{\mathbf{T_{old} - T_{old,min}}}{\mathbf{T_{old,max} - T_{old,min}}} \quad \text{.....(7)}$$

where

$\mathbf{T_{old,max}}$, $\mathbf{T_{old,min}}$ are the max and min input values of inputs variables, whereas $\mathbf{T_{old}}$, $\mathbf{T_{new}}$ are the values of old and new variables, respectively.

Model Learning

Artificial Neural Network Methodology

The algorithm of backpropagation in neural networks consists of the following sequence (Lek and Guégan, 1999):

- The number of nodes (input, hidden, and output layer) is set relative to the number of input and out.
- Learning rates and the maximum iterations (set all weights and thresholds to small random values) are initialized.
- The activation function which interconnects input neuron to it is output by a mathematical equation.
- Input values for the hidden nodes are determined based on Eq. 8:

$$\mathbf{S_j} = \sum_{\mathbf{i=1}}^{\mathbf{n}} \mathbf{X_i W_{ij}} \quad \text{.....(8)}$$

where $\mathbf{X_i}$ is the input variable at the node I and $\mathbf{W_{ij}}$ is the weight from input node i to hidden node j.

Table 2: ANN dataset input parameters

No.	Authors	Model Type	Objective Function	Ignored parameters
1	Usman et al., (1984)	3D and 2D Model	• Vertical fracture height • Fracture half-length • Fracture width	• Artificial Barrier mass proppant • Artificial Barrier Proppant Pack permeability • Proppant type
2	Fung et al., (1987)	Mathematical Model	• Vertical fracture height	• Artificial Barrier mass proppant • Artificial Barrier Proppant Pack permeability • Proppant type
3	Rahim et al., (1993)	Mathematical Model	• Vertical fracture height • Fracture half-length • Fracture width • Dimensionless fracture conductivity	• Artificial Barrier mass proppant • Artificial Barrier Proppant Pack permeability • Proppant type
4	Yang et al., (2011)	Pseudo-3D Model	• Vertical fracture height • Fracture half-length • Fracture width	• Artificial Barrier mass proppant • Artificial Barrier Proppant Pack permeability • Proppant type
5	Garavand et al., (2018)	Modified Pseudo-3D (LEFM and 2D-UFD) Model	• Vertical fracture height • Fracture half-length • Fracture width	• Artificial Barrier mass proppant • Artificial Barrier Proppant Pack permeability • Proppant type
6	Present work	ANN	• Vertical fracture height • Fracture half-length • Dimensionless fracture conductivity	

Table 3 : Real field data range for 59 fracture treatment

Parameter	Min.	Max.	Parameter	Min.	Max.
pay zone in-situ stress	3872	14465	Upper Layer 2 Toughness	700	2400
Main Mass Prop, 1000 Lb	38.6	121.6	Main treatment Pumping Rate, BPM	20	30
Lower Layer 1 in-situ stress	3872	14465	Upper Layer 1 permeability, md	0.001	25
Net Pressure, psi	450	2152	Rheology flow behavior index, n'	0.11	0.54
Upper Layer 1 in-situ stress	3872	14465	Rheology consistency index, K'	0.035	0.150
Upper Layer 1 Toughness	700	2400	Fracture gradient	0.65	1.16
pay zone E', *E+6	2.2	3.1	Lower Layer 1 permeability, md	0.001	25
Upper Layer 1 E', *E+6	1.28	5.66	Net pay formation thickness, ft	4.8	84
Upper Layer 2 permeability, md	0.001	25	Reservoir Pressure, psi	1500	6100
Barrier Mass Prop, 1000 Ib	10	16.5	Upper Layer 2 in-situ stress	3872	14465
pay zone permeability, md	2	70	Lower Layer 1 Toughness	700	2400
Pay zone Toughness	700	2400	Artificial Barrier Proppant Pack permeability, md *E+5	2.1	3.05

Table 3 Real field data range for 59 fracture treatment (cont.)

Parameter	Min.	Max.	Parameter	Min.	Max.
Lower Layer 2 in-situ stress	3872	14465	Reservoir Porosity %	7.8	26
Formation Lithology	1	5	Leak-off coefficient (CL), (ft/min½)* E-3	1.96	8.25
Distance to WOC, ft	16	171	Spurt loss coefficient (Sp), gal/100 ft2	0.5	2
Reservoir Temperature, F°	175	290	Upper Layer 1 Lithology	1	5
Upper Layer 1 Thickness	2	74	Upper Layer 2 Thickness	2	74
Upper Layer 2 Lithology	1	5	Main fracture Type	1	2
Barrier proppant type	1	2	Barrier proppant concentration, PPA	0.5	2
Closure gradient	0.55	0.78	Lower Layer 2 Toughness	700	2400
Lower Layer 2 permeability, md	0.001	25	Lower Layer 2 Thickness	2	74
Lower Layer 2 Lithology	1	5	Lower Layer 1 Lithology	1	5
Lower Layer 1 Thickness	2	74	Lower Layer 2 Toughness	700	2400
Lower Layer 1 E', *E+6	1.28	5.66	Lower Layer 2 E', *E+6	1.28	5.66

, Then the output was derived from the hidden nodes according to Eq. 9:

$$\mathbf{Y_j} = \mathbf{f(S_j)} = \frac{1}{1+e^{-S_j}} \quad \text{.....(9)}$$

where $\mathbf{Y_j}$ is the output variable from hidden node j. The same algorithm was employed to calculate the inputs to the output nodes.

- The error term for the output node was calculated.
- Iteration ending condition was defined when the network errors were larger than a predetermined threshold or the number of iterations was less than the maximum preset iterations, then the calculation process continued till one of these criteria was achieved.

In this study, a simple three-layered ANN network (one input layer, one hidden layer, and one output layer) was created by programming software MATLAB™ to be suitable for this amount of input data. A cross-validation plot was applied to determine The most proper number of neurons in the hidden layer. It is clearly shown that the highest R value was achieved when the number of neurons in the hidden layer was 61 neurons.

Weights and biases of the network were then appropriately initialized and therefore the artificial neural network was subjected to a backpropagation training algorithm (Mutalova *et al.*, 1996). ANN training and testing data involve the use of a total of 59 points, 40 datasets (70% of original data sets) are used for ANN training while the other 19 datasets (30% of original datasets) are used for model verification and testing. Table 4 illustrate the summary of artificial neural network data.

Table 4 :Neural Network parameters.

Network structure	ANN parameter
Input layer neurons	49
Output layer neurons	3
Hidden layer	1
Hidden layer neurons	61
Activation function	Sigmoid (Tan-Sig) &
Learning rate	Linear
	0.001

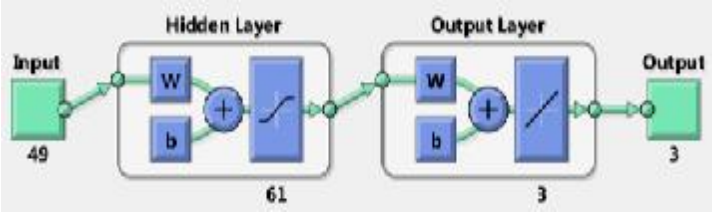

Fig. 3- The proposed ANN model architecture (Generated by MATLAB ™).

Artificial Neural Training

The ANN model was trained by backpropagation method by learning rate 0.001. Fig. 3 presents the structure of the proposed ANN model used in this study with 49 input parameters and one hidden sigmoid layer with 61 neurons across this layer, then 3 outputs through a linear output layer.

Appendix A illustrates the proposed ANN training script. The correlation coefficient (R) for whole data matches 0.93 is considered acceptable to complete the learning process of this model. This value was calculated through 46 iteration that calculates the correlation coefficient output error for each lesson. Fig. 4 shows the regression analysis of the trained ANN model.

Model Evaluation

The accuracy of the neural network model is evaluated by using validation and testing data through several statistical error analysis including Mean Squared Error (MSE), Correlation Coefficient (R), Standard Deviation (SD), Root Mean Squared Error (RMSE), Average Percent Relative Error (APRE) and Average Absolute Percent Relative Error (AAPRE) (Fath *et al.*, 2018 & Elgibaly and Osman, 2019). These statistical error analysis can be calculated as follow:

1) Average percent relative error (APRE)

$$\mathbf{APRE} = \frac{1}{n}\sum_{i=1}^{n} \text{APRE}\ \% \quad \text{.....(10)}$$

Where

$$\mathbf{APRE}\ \% = \left(\frac{X_{act.} - X_{pred.}}{X_{act.}}\right)_i \times 100, \quad i = (1,2,3 \ldots\ldots, n)$$

……..(11)

where $X_{act.}$ and $X_{pred.}$ are the actual value and predicted values from the model, respectively, and n is the number of the total dataset.

Average absolute percent relative error (AAPRE)

$$\mathbf{AAPRE} = \frac{1}{n}\sum_{i=1}^{n}|\text{AAPRE }\%| \quad \text{.....(12)}$$

Root mean square error (RMSE)

$$\mathbf{RMSE} = \sqrt{\frac{1}{n}\sum_{i=1}^{n}\left(X_{act.} - X_{pred.}\right)^2} \quad \text{.....(13)}$$

2) Mean Square Error (MSE)

$$\mathbf{MSE} = \frac{1}{n}\sum_{i=1}^{n}(target_i - output_i)^2 \quad \text{.....(14)}$$

where target and output are the actual value and predicted values from model, respectively, and n is the number of the dataset.

3) Standard Deviation (SD)

$$\mathbf{SD} = \sqrt{\frac{1}{n-1}\sum_{i=1}^{n}\left(\frac{X_{act.} - X_{pred.}}{X_{act.}}\right)^2} \quad \text{.....(15)}$$

4) Correlation Coefficient (R)

$$\mathbf{R} = \sqrt{1 - \frac{\sum_{i=1}^{n}\left(X_{act.} - X_{pred.}\right)^2}{\sum_{i=1}^{n}(X_{act.} - \bar{X})^2}} \quad \text{.....(16)}$$

Where $\bar{X}$ is the average actual values and can express as follows:

$$\bar{\mathbf{X}} = \frac{1}{n}\sum_{i=1}^{n}\mathbf{X_{act.}} \quad \text{.....(17)}$$

Statistical analysis values of the proposed ANN model for the prediction of fracture half-length, fracture height, and dimensionless fracture conductivity are listed in Table 5.

One of the strongest methods for ANN model performance evaluations is AAPRE. As is evident from Table 5, the proposed ANN model with AAPRE of 28.9% has a better efficiency compared to commercial software with AAPRE 43.07 %. Besides, the proposed ANN exhibited the highest correlation coefficients 0.902 compared to commercial software 0.86. The higher accuracy of the proposed ANN model confirms that this model was successfully trained.

Root Mean Square Error (RMSE) is another indicator of the rigidity of the proposed ANN model, as is obvious from Table 5, the proposed ANN model can provide a small value of RMSE rather than commercial software. So, from different statistical error analysis, the proposed ANN model outperforms the commercial software.

Table 5 : ANN statistical error analysis comparison

	Software Error Calculation						ANN Error Calculation					
Frac Parameter	APRE %	AAPRE %	RMSE	MSE	SD	R	APRE %	AAPRE %	RMSE	MSE	SD	R
Height, Hf	-14.06	43.07	44.9	2023.38	0.5	0.86	-11.4	28.9	40.2	1621.7	0.38	0.902
Half length, Xf	0.829	32.71	92.2	8506.16	0.3	0.88	10.3	19.8	62	3845.3	0.24	0.924
FCD	-6247.7	6247.7	532.1	283152	78.4	0.19	-0.51	60.2	7.7	60.241	0.81	0.891

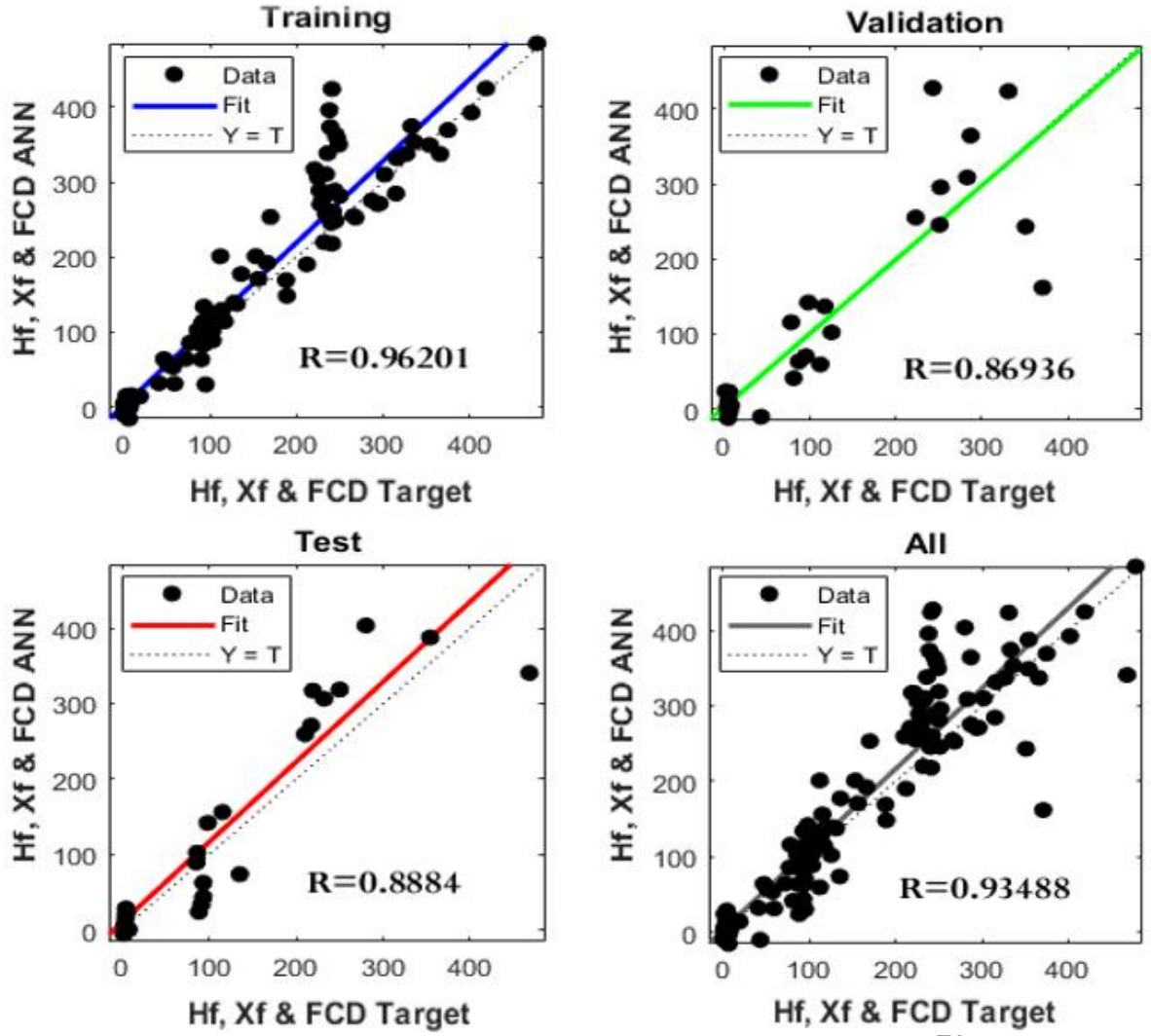

Fig. 4- Regression of the proposed ANN model (Generated by MATLAB ™).

RESULT AND DISCUSSION

ANN model structure

The total data set was divided into three data sets: training set, validation set, and testing set. More specifically, 30% of the whole dataset was randomly selected as the testing and validation sets and then utilized for comparison between the proposed ANN model and commercial software.

This ANN is developed using the parameters provided in Table 2. One hidden layer is constructed, and the hidden layer has 61 neurons. Fig. 4 depicts the prediction results of the regression analysis for training, validation, testing, and all data.

It is found that the difference in a correlation coefficient (R) between training and testing data sets is relatively small, which indicates that the ANN model training process is reliable.

Moreover, it can be observed that the predicted fracture height, half-length, and FCD have a good match with the target values with an acceptable range of accuracy. The R of testing data set is estimated to be 0.88 indicating that the ANN model has a relatively strong predictive performance.

A more statistical analysis values calculations are listed in Table 5. As can be seen that the standard deviation (SD) and correlation coefficient of the aforementioned dataset for fracture

height are 0.38 and 0.0.902 respectively. The average correlation coefficient for all the three outputs is 0.962 for training, 0.869 for validation, and 0.888 for testing, respectively.

Comparison between ANN predicted data and commercial software

The output parameters for fracture height, half-length, and fracture dimension-less conductivity were calculated by commercial software, then compared with ANN proposed model. The validation and test data around 18 real cases were used for this comparison.

Fig. 7 shows The cross plots of ANN and FracCade™ output parameters. It is observed that the ANN output parameters (fracture height, half-length, and FCD) have more accuracy rather than commercial software outputs. Table 5 illustrate the error comparison between ANN and software. It is shown also that the ANN was less error compare to well test data than commercial software due to the following reasons:-

- ANN model trained based on real well test data for different treatment jobs and at different formations of the western desert of Egypt rather than simulated stress profile for different commercial software, therefore model will achieve the highest accuracy than FracCade™ software.
- Besides, the ANN model includes harmonic average permeability approach (Kantzas *et al.,* 2012) for calculated dimensionless fracture conductivity as it considers that the total pressure drop is equal to the sum of pressure drop across each bed Fig. 8, so there was a big difference between ANN and commercial software error results Fig. 7 (c,f).

$$\Delta \mathbf{p} = \Delta \mathbf{p_1} + \Delta \mathbf{p_2} + \Delta \mathbf{p_3} \quad \text{(18)}$$

$$\frac{\mathbf{q\mu L}}{\mathbf{AK_{avg}}} = \frac{\mathbf{q\mu L_1}}{\mathbf{AK_1}} + \frac{\mathbf{q\mu L_2}}{\mathbf{AK_2}} + \frac{\mathbf{q\mu L_3}}{\mathbf{AK_3}} \quad \text{(19)}$$

and

$$\mathbf{K_{avg}} = \frac{\sum_{i=1}^{n} \mathbf{L_i}}{\sum_{i=1}^{n} (\frac{\mathbf{L}}{\mathbf{K}})_i} \quad \text{(20)}$$

where q is the flowrate of the formation, k is the permeability of the formation, A is the cross-sectional area of the formation and μ is the viscosity of the fluid

- ANN will calculate effective fracture half-length and actual dimensionless fracture conductivity FCD, however, any commercial software will calculate either total fracture half-length or propped half-length and simulated FCD.
- Integration between hydraulic fracture design, mini frac analysis, and well test data will give more confidence for the model compared to any commercial software.

BoxPlot parameter effect

The conventional data analysis such as plotting of each parameter versus the output was found to be very difficult to explain the relationship between the input parameters and the outputs. Therefore, a boxplot was used to identify this relationship (Mohamed *et al.,* 2019). Fig. 9 presents the relationship between several rock properties, hydraulic fracture treatment parameters and artificial barrier parameters with fracture height growth.

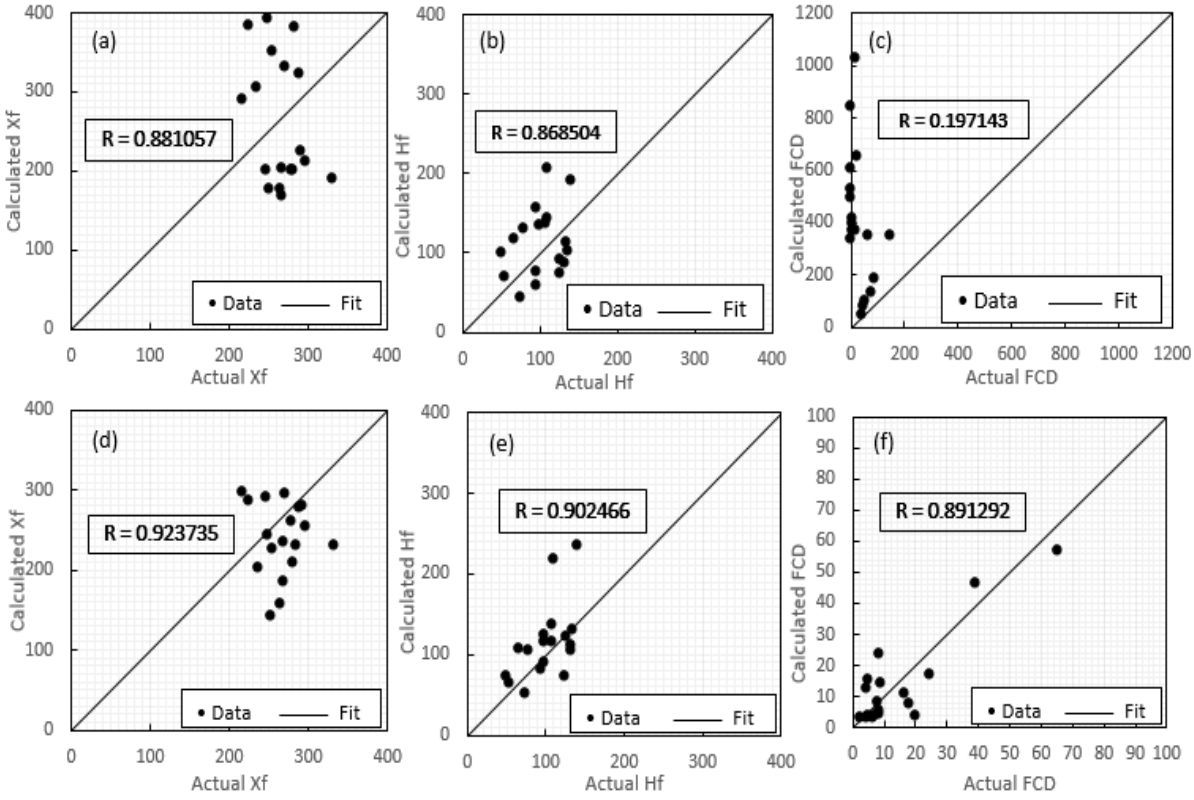

Fig. 7-ANN and Software comparison for fracture height, fracture half-length and fracture conductivity. (a) Software fracture half-length; (b) Software fracture height; (c) Software fracture conductivity; (d) ANN fracture half-length; (e) ANN fracture height; (f) ANN fracture conductivity.

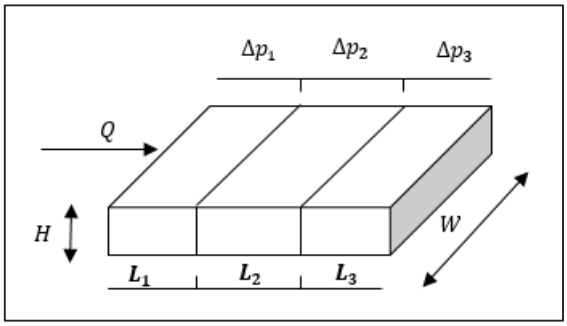

Fig. 8- Harmonic average permeability (Kantzas *et al.*, 2012).

Several interesting observation was mentioned. First, Fig. 9 -a, b, d, and f illustrate that fracture height increased with the increase of pumping rates, main treatment mass volume, artificial barrier proppant type, and fluid rheology flow behavior presented in fluid gel loading respectively.

Second, Fig. 9-c and e illustrate that fracture height decreased with the increase of permeability and stress contrast between overlying and underlying formations.

Fig 9-a shows greater fracture height with increasing pumping rates. Once the formation in situ stress is overcome and fracture initiation happens, the pump rate must be adequate to overcome the natural formation leak-off rate just to keep the fracture open. An additional pump rate is then needed to increase downhole pressure and promote further propagation of the fracture.

Fig. 9-b shows a greater fracture height with increasing proppant mass volume. This means that as long as proppant mass volume was increased, the fracture height will grow into unwanted zones and cannot be containment.

When the fracture grows into a formation of high permeability (high leak-off), it will be impossible for the hydraulic fracture geometry to penetrate through this formation. Fig. 9-c illustrates that as the formation permeability contrast between upward and downward zones increases the fracture height will be decreased.

For more fracture height containment, high-density proppant was pumped before the main hydraulic fracturing treatment with high breaker concentration. This bank will help in arresting the downward movement of the fracture height to unwanted formations by increasing the in-situ stress differential above the unwanted zone (Garcia *et al.*, 2001 & Mukherjee *et al.*,1995). Fig. 9-d shows that smaller proppant mesh the size will create a smaller value for proppant pack permeability. Therefore, developed more resistance for the main fracture treatment movement lead to increase half-length rather than fracture height.

Depending on the formation stresses fracture height growth is controlled by regulating the pump injection rates or using a fluid with low viscosities to avoid exceeding a critical pressure that may cause excessive unwanted fracture height propagation the pay zone Warpinski *et al.*, (1981). Fig. 9-e illustrates that one of the main parameters for fracture height containment is that the barrier in-situ stresses the contrast between the pay zone and the upward and downward formation layers.

Fig. 9-f shows that decreasing fracture fluid viscosity leads to decreasing the net pressure, then decreasing the ratio of pnet/ $\Delta\sigma$ Simonson *et al.*, (1978). This concept enables better arresting of fracture height growth to the unwanted formation, thus increasing effective fracture half-length in the pay zone. The consistency and stability test was validated by the rheology test for different gel loading concentrations to ensure that we have the proper one.

Garson Algorithm

Garson (Elgibal and Elkamel, 1998 & Zhou et al.,2015) introduce a method of partitioning the neural network connection weights to determine the relative importance of various input variable within the network. The connection weight of the ANN was utilized to determine the importance of each parameter.

The details of Garson algorithm are given by the following equation:

$$\mathbf{IM}(\mathbf{X_p}) = \frac{\sum_{j=1}^{n_h}\left[\left(|\mathbf{I}|_{p_j} \Big/ \sum_{K=1}^{n_p}|\mathbf{I}|_{p_j,K}\right)|\mathbf{O}|_j\right]}{\sum_{i=1}^{n_p}\left(\sum_{j=1}^{n_h}\left[\left(|\mathbf{I}|_{p_j} \Big/ \sum_{K=1}^{n_p}|\mathbf{I}|_{p_j,K}\right)|\mathbf{O}|_j\right]\right)} \quad \text{.....(21)}$$

Where $\mathbf{IM}(\mathbf{X_p})$ represents the percentage of influence of the input variable on the output. $\mathbf{n_p}$ is the number of input parameters and $\mathbf{n_h}$ is the number of neurons in the hidden layer. The term $|\mathbf{I}|_{\mathbf{p_j}}$ is the absolute value of the weight in the neural network for the $\mathbf{P_{th}}$input variables and $\mathbf{J_{th}}$ hidden layer. The term $|\mathbf{O}|_{\mathbf{j}}$ is the absolute value of the output layer weight in the neural network for $\mathbf{J_{th}}$ hidden layer.

Table 6 presents the relative importance of various input parameters on fracture height output from the ANN model.

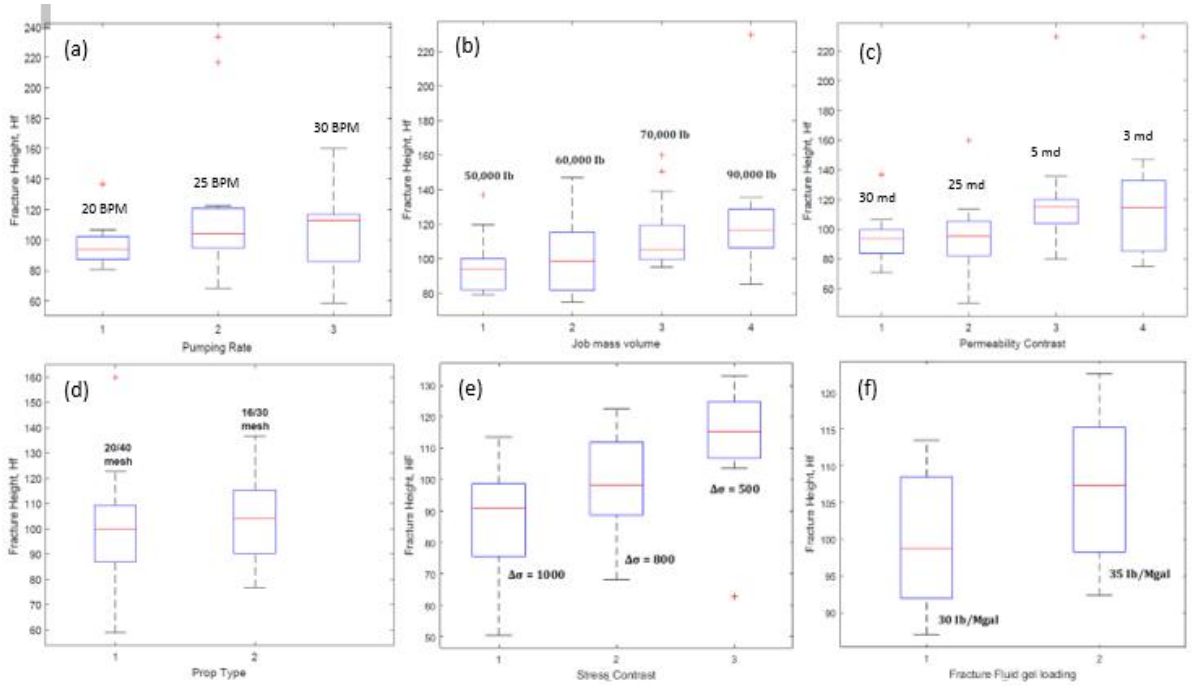

Fig. 9-Boxplots of effects of fracture stimulation parameters and rock properties on fracture height growth. (a) Pumping Rate; (b) Job mass volume; (c) Permeability contrast; (d) artificial barrier prop type; (e) stress contrast; (f) Fracture fluid gel loading (Generated by MATLAB ™).

Table 6: Relative importance of various input parameter in ANN model

Parameter	Relative importance (%)	Parameter	Relative importance (%)
Main Mass Prop	8.960	pay zone E'	2.233
pay zone in-situ stress	7.548	Upper Layer 1 Toughness	2.072
Lower Layer 1 in-situ stress	6.335	Upper Layer 2 permeability	1.911
pay zone permeability	5.635	Rheology flow behavior index, n'	1.851
Upper Layer 1 in-situ stress	3.423	Barrier Mass Prop	1.850
Main treatment Pumping Rate	3.323	Fracture gradient	1.829
Lower Layer 1 permeability	3.110	Upper Layer 2 Toughness	1.768
Net Pressure	3.073	Closure gradient	1.736
Reservoir Pressure	2.998	Rheology consistency index, K'	1.731
Upper Layer 1 permeability	2.986	Lower Layer 1 E'	1.715
Pay zone Toughness	2.552	Lower Layer 1 Toughness	1.475
Artificial Barrier Proppant Pack permeability	2.339	Upper Layer 2 in-situ stress	1.414

Table 6: Relative importance of various input parameter in ANN model (cont.)

Parameter	Relative importance (%)	Parameter	Relative importance (%)
Lower Layer 2 in-situ stress	1.411	Reservoir Porosity	0.981
Barrier proppant concentration	1.405	Distance to WOC	0.978
Leak-off coefficient (CL)	1.399	Spurt loss coefficient (Sp)	0.971
Reservoir Temperature	1.375	Upper Layer 1 Lithology	0.969
Upper Layer 1 Thickness	1.346	Upper Layer 2 Thickness	0.966
Upper Layer 1 E'	1.332	Main fracture Type	0.855
Barrier proppant type	1.291	Lower Layer 2 Toughness	0.825
Net pay formation thickness	1.284	Upper Layer 2 Lithology	0.811
Lower Layer 2 permeability	1.260	Lower Layer 2 Thickness	0.801
Lower Layer 2 Lithology	1.260	Lower Layer 1 Lithology	0.799
Lower Layer 1 Thickness	1.226	Lower Layer 2 Toughness	0.778
Formation Lithology	1.101	Lower Layer 2 E'	0.777

These results indicate that each input plays a great role in controlling fracture height according to each input weight, therefore optimizing hydraulic fracture design. In-situ stress contrast has a great contribution percent, followed by permeability contrast, fracture treatment proppant mass, net pressure value, artificial barrier proppant volume, and pack permeability, Young's modulus, fracture toughness, and pumping rate.

Garson results in table 6 can easily answer the following equation:

- How many parameters have a vital role in limiting the fracture height growth?
- What is the magnitude of contributions for each parameter in controlling fracture height?
- what can cause fracture height containment?

The results of the Garson calculation can be summarized as follows:

- Artificial barrier proppant pack permeability shows a relatively influence as proppant material will increase the in-situ stress contrast, therefore control fracture height growth.
- Artificial barrier proppant mass volume has a relative impact on frac height growth but the great impact on fracture half-length. A full-length barrier placement yields the max effective fracture half-length, though it is impossible to place.
- Fracture toughness can have a very significant impact on fracture growth. Consequently, contrasts in fracture toughness can form the most reliable barriers to height growth.
- The effect of young's modulus seems to be less important. A higher modulus layer tends to has a hindering effect when a fracture is approaching, whereas a lower modulus layer hinders the fracture height growth when the fracture in it.
- Garson's results reflect the importance of net fracture pressure, so by reducing net fracture pressure (Pnet), will help to control fracture height growth (Talbot *et al.*, 2000).

$$\mathbf{Pnet} = \Delta\mathbf{P} \approx \left[\frac{\mathbf{E}^{2\mathbf{n}'+}\ \mathbf{K}\ \mathbf{Q}^{\mathbf{n}'}\mathbf{L}}{(\mathbf{1}-\mathbf{v}^{\mathbf{2}})^{2\mathbf{n}'+}\ \mathbf{H}^{3\mathbf{n}'+}}\right]^{\frac{\mathbf{1}}{2\mathbf{n}'+}} \quad \text{.....(22)}$$

where E is Young's Modulus, n´ and k´ are Power Law fluid coefficients, Q is fluid injection rate, L is fracture length, $\boldsymbol{\nu}$ is Poisson's ratio, and *H* is fracture height.

Some mechanisms to achieve this objective are:

- Decreasing fracturing fluid viscosity by reducing fluid gel loading or using viscoelastic surfactant based fracturing fluids, or slickwater fracturing fluids that will be decreasing the fracture net pressure, therefore control fracture height.

- Using the Pillar fracturing technique with less pad volume and pumping rate would yield fewer net pressures compared to conventional fracturing treatment techniques.
- Decreasing frac treatment pumping rate (Decreasing Pnet).

CONCLUSION

Utilization of the ANN approach for predicting the fracture height growth, therefore optimizing the fracture geometry and conductivity has been investigated in the present study. The ANN model has been applied on a total of 59 real field data sets obtained from the western desert of Egypt and west of Nile fields. The model was composed of several rock properties for different types of reservoirs and different hydraulic fracture techniques either by different pumping technique (Conventional or channel frac) or various products (frac fluid or proppant type).

Transient well test analysis data is applied also to improve the accuracy of the ANN model, then the Garson algorithm is used to conduct the multi-factor analysis. Based on the process, some conclusions can be drawn as follows:

- New reliable Artificial Neural Network model trained based on real well test data for different treatment jobs, at different formations of the western desert of Egypt and west of Nile fields and for different reservoirs has been developed. The model utilizes better accuracy when compared with commercial software Table 5.
- ANN was applied to perform the multi-factor analysis. Results showed that stress contrast, permeability contrast, artificial barrier proppant mass and back permeability, main fracture treatment proppant mass volume, and pumping rate are the main factors, significantly affecting the fracture geometry and conductivity. Therefore, the aforementioned factors should be focus to optimize the fracture treatment in the actual situation.
- The artificial neural network model proved through Garson's calculation results the vital role for artificial barrier technology for either control fracture height growth into the underlying unwanted water-bearing zone or increasing the effective fracture half-length to maximize well productivity.
- The application of the ANN model in the estimation of effective FCD showed a good correlation coefficient of about 0.89, since it accounts for the harmonic average permeability approach, whereas the commercial software showed 0.197 Fig. 7-c, f.
- ANN will provide the effective fracture half-length and actual dimensionless fracture conductivity FCD, however, any commercial software will calculate either total fracture half-length or propped half-length and simulated FCD.
- Lacking detailed geomechanical properties, the ANN model is the best candidate for fracture design. In such a case, the additional effort to run a simulation run with commercial software is not rewarded with higher accuracy in predicting fracture geometry if critical input parameters are unknown. In particular, in cases that close to water-bearing zones.
- The capability of the ANN model has been significantly improved by increasing hydraulic fracturing jobs, therefore increase model efficiency.

In future work, applying the radial basis activation function (Salem *et al.*, 2018) to predict fracture geometry and conductivity, then compare the result with the multi-layer perceptron (MLP) algorithm till getting the accurate neural model that depicts the fracture dimensionless conductivity, half-length, and fracture height.

REFERENCES

Ahmed, U., 1984, January. A practical hydraulic fracturing model simulating necessary fracture geometry, fluid flow and leak off, and proppant transport. In SPE Unconventional Gas Recovery Symposium. Society of Petroleum Engineers.

Ahn, C.H., Dilmore, R. and Wang, J.Y., 2017. Modeling of hydraulic fracture propagation in shale gas reservoirs: a three-dimensional, two-phase model. ASME J. Energy Resour. Technology, 139(1), p.012903.

Beale, H.D., Demuth, H.B. and Hagan, M.T., 1996. Neural network design. PWS Publish Company, 11, pp.1-47.

Economides, M., Oligney, R. and Valkó, P., 2002. Unified fracture design, chapter- 8: bridging the gap between theory and practice. Orsa Press.

Elgibaly, A. and Osman, M.A., 2019. Perforation friction modeling in limited entry fracturing using artificial neural network. Egyptian Journal of Petroleum, 28(3), pp.297-305.

Elgibaly, A.A. and Elkamel, A.M., 1998. A new correlation for predicting hydrate formation conditions for various gas mixtures and inhibitors. Fluid Phase Equilibria, 152(1), pp.23-42.

Elkatatny, S., 2018. Application of Artificial Intelligence Techniques to Estimate the Static Poisson's Ratio Based on Wireline Log Data. ASME J. Energy Resour. Technology, 140(7), p.072905.

Fath, A.H., Madanifar, F. and Abbasi, M., 2018. Implementation of multilayer perceptron (MLP) and radial basis function (RBF) neural networks to predict solution gas-oil ratio of crude oil systems. Petroleum.

Fung, R.L., Vilayakumar, S. and Cormack, D.E., 1987. Calculation of vertical fracture containment in layered formations. SPE formation evaluation, 2(04), pp.518-522.

Garavand, A. and Podgornov, V.M., 2018. Hydraulic fracture optimization by using a modified Pseudo-3D model in multi-layered reservoirs. Journal of Natural Gas Geoscience, 3(4), pp.233-242.

Garcia, D.G., Prioletta, A. and Kruse, G.F., 2001, January. Effective control of vertical fracture growth by placement of an artificial barrier (Bottom Screen Out) in an exploratory well. In SPE Latin American and Caribbean Petroleum Engineering Conference. Society of Petroleum Engineers.

Kantzas, A., Bryan, J. and Taheri, S., 2012. Fundamentals of fluid flow in porous media. Pore size distribution, chapter- 2.

Lek, S. and Guégan, J.F., 1999. Artificial neural networks as a tool in ecological modelling, an introduction. Ecological modelling, 120(2-3), pp.65-73.

Mendelsohn, D.A., 1984. A review of hydraulic fracture modeling—II: 3D modeling and vertical growth in layered rock. ASME J. Energy Resour. Technol, 106(4), pp.543-553.

Mohamed, I.M., Mohamed, S., Mazher, I. and Chester, P., 2019, September. Formation Lithology Classification: Insights into Machine Learning Methods. In SPE Annual Technical Conference and Exhibition. Society of Petroleum Engineers.

Mukherjee, H., Paoli, B.F., McDonald, T., Cartaya, H. and Anderson, J.A., 1995. Successful control of fracture height growth by placement of artificial barrier. SPE Production & Facilities, 10(02), pp.89-95.

Mutalova, R.F., Morozov, A.D., Osiptsov, A.A., Vainshtein, A.L., Burnaev, E.V., Shel, E.V. and Paderin, G.V., 2019. Machine learning on field data for hydraulic fracturing design optimization. arXiv preprint arXiv:1910.14499.

Palmer, I.D. and Luiskutty, C.T., 1986. Comparison of Hydraulic Fracture Models for Highly Elongated Fractures of Variable Height. ASME J. Energy Resour. Technology, 108(2), pp.107-115.

Pitakbunkate, T., Yang, M., Valko, P.P. and Economides, M.J., 2011, January. Hydraulic fracture optimization with a p-3D model. In SPE Production and Operations Symposium. Society of Petroleum Engineers.

Rahim, Z. and Holditch, S.A., 1993, January. Using a Three-Dimensional Concept in a Two-Dimensional Model To Predict Accurate Hydraulic Fracture Dimensions. In SPE Eastern Regional Meeting. Society of Petroleum Engineers.

Salah, M., Gabry, M.A., ElSebaee, M. and Mohamed, N., 2016, November. Control of hydraulic fracture height growth above the water zone by inducing an artificial barrier in Western Desert, Egypt. In Abu Dhabi International Petroleum Exhibition & Conference. Society of Petroleum Engineers.

Salem, A., Elgibaly, A., Attia, M. and Abdulraheem, A., 2018, August. Comparing 5-Different Artificial Intelligence Techniques to Predict Z-Factor. In SPE Kingdom of Saudi Arabia Annual Technical Symposium and Exhibition. Society of Petroleum Engineers.

Simonson, E.R., Abou-Sayed, A.S. and Clifton, R.J., 1978. Containment of massive hydraulic fractures. Society of Petroleum Engineers Journal, 18(01), pp.27-32.

Talbot, D.M., Hemke, K.A. and Leshchyshyn, T.H., 2000, January. Stimulation fracture height control above water or depleted zones. In SPE Rocky Mountain Regional/Low-Permeability Reservoirs Symposium and Exhibition. Society of Petroleum Engineers.

The Egyptian General Petroleum Corporation, 1992. Western desert oil and gas fields (A comprehensive overview). EGYPT.

Warpinski, N.R., Clark, J.A., Schmidt, R.A. and Huddle, C.W., 1981. Laboratory investigation on the effect of in situ stresses on hydraulic fracture containment (No. SAND-80-2307C; CONF-810518-5). Sandia National Labs., Albuquerque, NM (USA).

Zhou, B., Vogt, R.D., Lu, X., Xu, C., Zhu, L., Shao, X., Liu, H. and Xing, M., 2015. Relative importance analysis of a refined multi-parameter phosphorus index employed in a strongly agriculturally influenced watershed. Water, Air, & Soil Pollution, 226(3), p.25.